



HAL
open science

Bi-anisotropic homogenization of metamaterials

Geoffroy Klotz, Nicolas Mallejac, Stefan Enoch

► **To cite this version:**

Geoffroy Klotz, Nicolas Mallejac, Stefan Enoch. Bi-anisotropic homogenization of metamaterials. 2020. hal-02533037

HAL Id: hal-02533037

<https://hal.science/hal-02533037>

Preprint submitted on 6 Apr 2020

HAL is a multi-disciplinary open access archive for the deposit and dissemination of scientific research documents, whether they are published or not. The documents may come from teaching and research institutions in France or abroad, or from public or private research centers.

L'archive ouverte pluridisciplinaire **HAL**, est destinée au dépôt et à la diffusion de documents scientifiques de niveau recherche, publiés ou non, émanant des établissements d'enseignement et de recherche français ou étrangers, des laboratoires publics ou privés.

Bi-anisotropic homogenization of metamaterials

Geoffroy Klotz*

*CEA DAM/Le Ripault, BP 16, F-37260 Monts, France and
Aix Marseille Univ, CNRS, Centrale Marseille, Institut Fresnel, Marseille, France*

Nicolas Malléjac†

CEA DAM/Le Ripault, BP 16, F-37260 Monts, France

Stefan Enoch

Aix Marseille Univ, CNRS, Centrale Marseille, Institut Fresnel, Marseille, France

(Dated: April 6, 2020)

Electromagnetic meta-materials composed of a 3-D lattice of small conducting resonators can be convenient to reach interesting permittivity and permeability levels, especially for applications such as invisibility cloaking or superlenses. In this article, we present a fast dipolar expansion of meta-atoms based on the far-field extracted from a simulation or experimentation. Using a dipole approximation of the field scattered by a single inclusion, we develop a homogenization method based on the Clausius-Mossotti relation, taking into account the interactions between meta-atoms. We then establish a generalization of the Clausius-Mossotti relation for bi-anisotropic meta-materials to extend our methodology to a more general class of meta-atoms. Some examples are given based on full-wave simulations of a meta-atom, and a comparison with other approaches allows an evaluation of the relevance of this methodology.

I. INTRODUCTION

Metamaterials are microstructured media exhibiting interesting physical behavior in many domains: electromagnetics, mechanics and thermodynamics. The use of metamaterials appears to be a privileged way to achieve specific electromagnetic devices, such as superlenses [1] or invisibility cloaks [2] [3]. The main objective consists in creating an artificial micro-structured medium that behaves in a specific way to reach electromagnetic effective properties that cannot be found in nature.

For superlenses, the property of interest is the refractive index, which has to be negative to achieve negative refraction. More specifically, for lossless materials, this means that we either have both negative permittivity and permeability at a given frequency. On the contrary, permittivity and permeability required for an invisibility cloak don't need to reach negative values. However, their realization remains very difficult because of the high anisotropy levels and high inhomogeneity needed in the cloak medium. Moreover, a theoretical invisibility cloak in free space always involves the use of Epsilon-Near-Zero (ENZ) and Mu-Near-Zero (MNZ) materials [2] [4] [5]. This allows the creation of a refractive index below unity, that is needed to divert the rays from their original trajectory without disturbing their phase.

The development of metamaterials allowing the production of such complex electromagnetic devices

relies on the homogenization methods used to determine their effective properties. Many papers have focused on the way to extract permittivity and permeability via the Nicolson-Ross methodology [6] [7] [8]. More recently, this method has been adapted to metamaterials [9] [10], whereas alternative ways to extract parameters have emerged [11] [12] [13], introducing a definition of effective permittivity and permeability parameters. Chirality and more generally bi-anisotropy is usually not taken into account in the classical methods, but have been observed many times in the study of metamaterials [14] [15] [16] and especially for the lattices of resonating structures. These effects, caused by the geometry of the inclusions, render the extraction of the classic permittivity and permeability parameters irrelevant because it provides crossed reactions between electric and magnetic excitations. The authors of these papers and of ref.[17] tried to take advantage of bi-anisotropic phenomena to create an effective negative refractive index for a given incident wave. Other authors suggest homogenization methodologies that take into account the specific behavior of the material and give chirality parameters in addition to a restored permittivity and permeability [18] [19] [20] [21].

Metamaterials composed of a lattice of resonating structures often exhibit complex behavior and 3D-simulations required for most homogenization methods lead to an important computational burden for both RAM and processors. An alternative approach consists in the study of the metamaterial through the analysis of the field scattered by a single particle. This approach has been developed in [22] [23] [24] [25] and constitutes a relevant way to analyse metamaterials that does not require a simulation of the whole lattice.

* geoffroy.klotz@cea.fr

† nicolas.mallejac@cea.fr

Based on this single meta-atom approach, we developed in a previous work [26] a fast extraction method of the electric and magnetic moments for a single particle in free space. Using a limited set of directions for the far-field, we easily obtain a two-orders multipole expansion. The scattering properties of the single-particle in free space give important clues to understand the physics of the whole metamaterial. We also briefly mentioned a homogenization methodology for permittivity and permeability based on the expansion of the field scattered.

In this article, we use a fast method to perform a dipole expansion of the meta-atoms, we give an example of inclusion studied through this approach and compare it to a more traditional method. Then, we propose an extension of this methodology to realize a full bi-anisotropic homogenization procedure based on a Clausius-Mossotti relation generalized to bi-anisotropic metamaterials. We finally validate our method thanks to a comparison with a theoretical approach developed in [27].

II. DIPOLE EXPANSION

Multipole expansion methods used to study the radiated far fields require a large number of extraction points from the simulation or the experimentation to perform a projection on a spherical harmonic basis and deduce the multipole moments. However, around its first frequency of resonance, the field scattered by a meta-atom is mainly dipolar [22] [26]. Considering that the field scattered by a meta-atom can be approximated by the sum of an electric and a magnetic dipole contribution, we describe in this section a fast method allowing the extraction of the dipole moments exhibited by a meta-atom using the extraction of the electric field along a very limited number of directions.

Considering that the first order of the expansion is preponderant and based on equations presented in [28], we can write the electric far-field \mathbf{E}_m scattered by a single meta-atom in free space:

$$\mathbf{E}_m = \frac{Z_0 c k^2}{4\pi} \frac{e^{ikr}}{r} [(\mathbf{n} \times \mathbf{p}) \times \mathbf{n} - \mathbf{n} \times \mathbf{m}/c] \quad (1)$$

with \mathbf{n} the unit vector in the direction of observation, Z_0 the free space impedance, k the free space wavenumber, r the distance between the evaluation point and the meta-atom, \mathbf{p} and \mathbf{m} , the electric and magnetic dipoles.

A simulation of the single meta-atom in free space is computed with a background linearly polarized plane wave. Thanks to this simulation we evaluate the far-field scattered by the meta-atom in an arbitrary direction described by its angular coordinates (θ, ϕ) . For example, if we choose $(\theta, \phi) = (0, 0)$, a projection along x, y and z-axis gives us the three following equations :

$$\begin{cases} \mathbf{E}_{\text{far}}(0, 0) \cdot \mathbf{x} = \frac{Z_0 c k^2}{4\pi} \frac{e^{ikr}}{r} (p_x - m_y/c) \\ \mathbf{E}_{\text{far}}(0, 0) \cdot \mathbf{y} = \frac{Z_0 c k^2}{4\pi} \frac{e^{ikr}}{r} (p_y + m_x/c) \\ \mathbf{E}_{\text{far}}(0, 0) \cdot \mathbf{z} = 0 \end{cases} \quad (2)$$

We obtain here two non-trivial equations linking the projections of the electric field to the variables of interest, the electric and magnetic dipole moments. The projection along z-direction is zero because the field propagates orthogonally to its orientation. Repeating this procedure with two other directions of extraction of the field, we can build a matrix equation by concatenation of the non-trivial equations :

$$\frac{4\pi r e^{-ikr}}{Z_0 k^2} \begin{pmatrix} E_y(\pi/2, 0) \\ E_z(\pi/2, 0) \\ E_x(\pi/2, \pi/2) \\ E_z(\pi/2, \pi/2) \\ E_x(0, 0) \\ E_y(0, 0) \end{pmatrix} = \begin{pmatrix} 0 & 1 & 0 & 0 & 0 & 1 \\ 0 & 0 & 1 & 0 & -1 & 0 \\ 1 & 0 & 0 & 0 & 0 & -1 \\ 0 & 0 & 1 & 1 & 0 & 0 \\ 1 & 0 & 0 & 0 & 1 & 0 \\ 0 & 1 & 0 & -1 & 0 & 0 \end{pmatrix} \begin{pmatrix} p_x \\ p_y \\ p_z \\ m_x/c \\ m_y/c \\ m_z/c \end{pmatrix} \quad (3)$$

A simple inversion of the 6-by-6 matrix then gives the dipole moments.

Although this methodology of dipole expansion of

a meta-atom is very general, we fixed as an example a geometry of inclusion to illustrate its interest. This geometry is presented in fig. 1: this inclusion is composed of a thin metallic rolled-up wire from which we

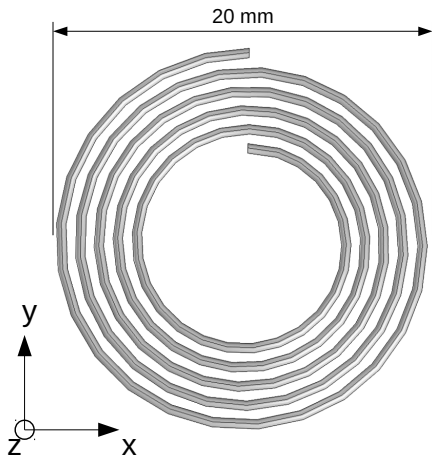


FIG. 1. Conductive flat spiral used as resonating structure for a 3D-metamaterial. The span of the particle is 20mm long whereas its curvilinear length is about 250mm long. We expect a low frequency resonance and a preponderant magnetic response.

expect a magnetic response. Indeed, the use of a highly curved metallic path should generate rotating currents along the surface and create an overriding dipolar magnetic response. Of course, we also expect a minor dipolar electric response. We also define an integral evaluation index to compare the dipole model and the field scattered by the particle according to the full-wave simulation.

$$I_{\text{model}} = \frac{\int_{\theta, \phi} \|\mathbf{E}_{\mathbf{m}} - \mathbf{E}_{\mathbf{ma}}\|^2 \sin(\theta) d\theta d\phi}{\int_{\theta, \phi} \|\mathbf{E}_{\mathbf{m}}\|^2 \sin(\theta) d\theta d\phi} \quad (4)$$

with $\mathbf{E}_{\mathbf{ma}}$ the exact field scattered by the meta-atom and θ and ϕ , respectively the polar and azimuthal angles in the spherical coordinate system.

The span of our inclusion is 2 centimeters long for a curvilinear length of 25 centimeters. We know from previous research [29] [30] that the longer the curvilinear length of the metallic path, the longer the free-space wavelength resonance. With a curvilinear wavelength that is one order of magnitude longer than the global span of the particle, we expect that the first resonance happens for a very long free-space wavelength compared to the span. Indeed if the particle is small compared to the wavelength it is easier to realize lattices of inclusions whose parameters are small enough to consider homogeneous behavior. The geometry of this structure can easily be represented and meshed with the COMSOL commercial software. The material used for the meta-atom is an electric conductor with a conductivity of $10^5 S/m$, which could correspond to graphene-based

composites in the microwave domain [31]. We did not choose a classical conductor like gold or copper because of their high conductivity. The resonance is much sharper at these levels of conductivity but we expect a smoother response of the material [12] [32].

Simulations are then made using the RF module in the frequency domain. To obtain a strong magnetic response, the magnetic field of the background wave is oriented along the z-axis and the electric field along the y-axis. The far-field is then extracted from the COMSOL file and sent to an algorithm that performs the dipole expansion. The results for our meta-atom are given in fig.2. As can be seen, the magnetic dipolar response is mainly oriented along the z-direction, which is the direction of the background magnetic field. The electric dipolar response is mainly oriented along the y-direction, that is the direction of the background electric field.

First, we confirm with the evaluation index that the hypothesis made on the far-field in equation 1 is verified: the evaluation index shows a maximum of the difference between the two-orders model and the far-field from the simulation of 0.16%, which is very low. We then consider that our expansion is valid and that it is relevant to neglect high order multipole moments. The most significant point in fig.2 is the comparison of the power radiated by the electric and the magnetic dipoles: we note that the magnetic dipolar moment is responsible for almost all the power radiated by the inclusion at the first frequency of resonance. This meta-atom could, therefore, be a good candidate for the realization of a magnetic metamaterial.

Note that even if the imaginary part of the electric dipole is positive, this metamaterial is actually passive. We have indeed to consider both electric and magnetic losses to conclude on the global passivity of the system [33].

III. MAGNETO-DIELECTRIC PARAMETERS EXTRACTION BY CLAUSIUS-MOSSOTTI INVERSION

Using the dipolar moments and the local electromagnetic fields, we can easily deduce the polarizability of the material composed of a lattice of the inclusion. The classical definition of the polarizability is given by :

$$\alpha_e = \frac{p}{\epsilon_0 E_l} \quad ; \quad \alpha_m = \frac{m}{H_l} \quad (5)$$

where E_l and H_l are the local electric and magnetic fields, whereas p and m are the electric and magnetic dipoles exhibited by the particle. In our simulations,

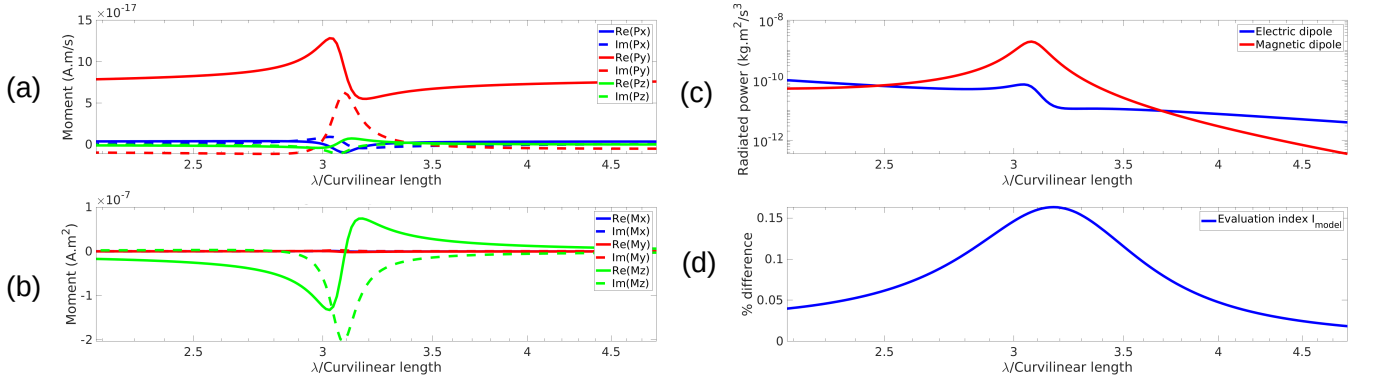


FIG. 2. Two-orders multipole expansion. The dipolar (a) (b) moments are given as functions of the reduced wavelength in free space. The corresponding radiated power (c) is also given for each moment. We observe a large preponderance of the dipolar magnetic moments at the first resonance of frequency. The magnetic response is mainly oriented in the z-direction, which is the direction of the magnetic excitation. The evaluation index (d) measures the difference between our two-orders model and the scattered far-field of the meta-atom, which remains under 0.16% over the whole frequency range.

the meta-atom is isolated so the local fields equal the background fields E_b and H_b of the plane wave. We consider in this section a diagonal permittivity and permeability tensor in the (x, y, z) basis and we also consider that no bi-anisotropic effect would make fields revolve. The constitutive equations that are assumed to describe the behavior of the material are given in equation 6:

$$\mathbf{D} = \epsilon_0 \begin{pmatrix} \epsilon_{r,xx} & 0 & 0 \\ 0 & \epsilon_{r,yy} & 0 \\ 0 & 0 & \epsilon_{r,zz} \end{pmatrix} \mathbf{E}$$

$$\mathbf{B} = \mu_0 \begin{pmatrix} \mu_{r,xx} & 0 & 0 \\ 0 & \mu_{r,yy} & 0 \\ 0 & 0 & \mu_{r,zz} \end{pmatrix} \mathbf{H}$$
(6)

The dielectric permittivity and magnetic permeability that we are looking for are the diagonal coefficients of respectively these permittivity and permeability matrices. We choose the electric field E_i to be oriented along x,y or z-axis. In a similar way, H_j is oriented along j-axis. Thanks to Clausius-Mossotti relations, we can link the electric polarizability of the meta-atom to the permittivity of a material composed of an assembly of this meta-atom. An analog of the Clausius-Mossotti relation for permeability can also be found in [34]:

$$\frac{\epsilon_{r,ii}(\omega) - 1}{\epsilon_{r,ii}(\omega) + 2} = \frac{1}{3\epsilon_0} N \alpha_{e,ii}(\omega)$$

$$\frac{\mu_{r,jj}(\omega) - 1}{\mu_{r,jj}(\omega) + 2} = \frac{\mu_0}{3} N \alpha_{m,jj}(\omega)$$
(7)

with N the density of particles, $\epsilon_{r,ii}(\omega)$ the relative permittivity along the i^{th} direction, $\mu_{r,jj}(\omega)$ the relative permeability along the j^{th} direction, $\alpha_{e,ii}(\omega)$ is

the electric polarisability and $\alpha_{m,jj}(\omega)$ the magnetic polarisability.

In our specific case, the density is given by the number of inclusion per unit of volume. This is given by the volume $V = a^3$ of the unit cell containing one inclusion, with a the lattice parameter of the cubic structure. The Clausius-Mossotti relation can, therefore, be written as a function of V , p_i and m_j and of the amplitude of background electric and magnetic fields.

$$\frac{\epsilon_{r,ii}(\omega) - 1}{\epsilon_{r,ii}(\omega) + 2} = \frac{p_i(\omega)}{3V\epsilon_0 E_i} \quad ; \quad \frac{\mu_{r,jj}(\omega) - 1}{\mu_{r,jj}(\omega) + 2} = \frac{m_j(\omega)}{3V H_j}$$
(8)

We previously considered that the electric excitation induces the electric response and that both have to be oriented in the same direction. Under this assumption, we can easily retrieve the effective permittivity and permeability, which are given by a simple inversion of the Clausius-Mossotti relations in equation 9.

$$\epsilon_{r,ii}(\omega) = \frac{1 + \frac{2p_i(\omega)}{3V\epsilon_0 E_i}}{1 - \frac{p_i(\omega)}{3\epsilon_0 V E_i}} \quad ; \quad \mu_{r,jj}(\omega) = \frac{1 + \frac{2m_j(\omega)}{3V H_j}}{1 - \frac{m_j(\omega)}{3V H_j}}$$
(9)

IV. EXAMPLE FOR A MAGNETIC METAMATERIAL

To verify the accuracy of the method based on the Clausius-Mossotti formula, we apply it on the small resonating metallic meta-atom represented in fig.1. A good test is to check if the results coming from our methodology are similar to results coming from the classical Nicolson-Ross method. For this purpose two kinds of simulations shown in fig.3 are performed.

First, we perform simulations where the inclusion is single in free space, with Perfectly Matched Layer (PML) standing for infinite space. A background polarized plane wave is defined and we realize a six-directions field extraction to have the two-orders multipole expansion (this methodology is described in parts 2 and 3). These simulations give the behavior of a single inclusion excited by a linearly polarized plane wave. As a rule of thumb, we consider that an evaluation index under 5% is necessary to neglect the contribution of higher multipole moments in the scattering properties of the particle. Then, if the evaluation index is small enough and the power emitted by the dipolar moments sufficiently important, we can use the permittivity and permeability calculation method.

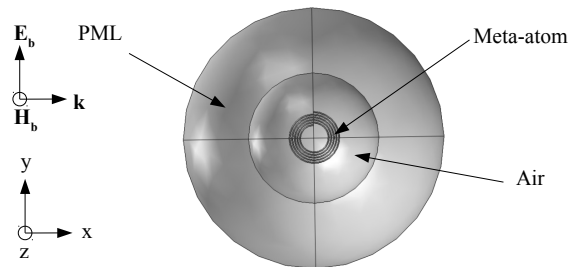
Then, we perform simulations that involve a whole lattice composed of the inclusion and supposed to behave as an homogeneous material. To perform such a simulation, we use periodic boundary conditions in two directions of space orthogonal to the direction of propagation. These simulations study six inclusions aligned in the direction of propagation of the incident wave. An emitting port plays the role of the electromagnetic source and sends a plane wave on the lattice of meta-atoms. On the opposite side, a receiving port allows the transmission of a plane wave. Using the Nicolson-Ross method, the extraction of the complex Fresnel coefficients yields the effective permittivity and permeability parameters. Simulations are performed over a frequency range around the first frequency of resonance. In this case, the frequency sweep was made starting from 0.25 GHz to 0.55 GHz with a step of 0.002 GHz, for a total of 151 different frequencies.

Fig.4 displays the results for a lattice parameter of 2.8 cm. The two methodologies give similar results and show that the response is mainly magnetic, as predicted with the multipolar expansion. The real part of the magnetic permittivity takes negative values around the frequency of resonance whereas the real part of the permeability is comprised between 1.2 and 1.6.

Many factors can explain the differences between the two methodologies. First, due to calculation considerations, we had to restrain the number of mesh elements. Thus, it may not be precise enough to describe the fine geometry of the meta-atom.

Then, the Clausius-Mossotti formula assumes a very high number of dipoles in the media in every direction of space. This hypothesis allows us to obtain an average value of the local electric field. In our simulation case, we set periodic boundary conditions in two directions. However, in the direction of the wave propagation, there are only six inclusions: the validity of the Clausius-Mossotti formula applied to such a thin lattice could be discussed. Moreover, the non-propagative field of a particle may have an impact on the neighbor particles.

3D-simulation of a single meta-atom in free space



3D-simulation of a lattice of meta-atoms with emitting and receiving ports

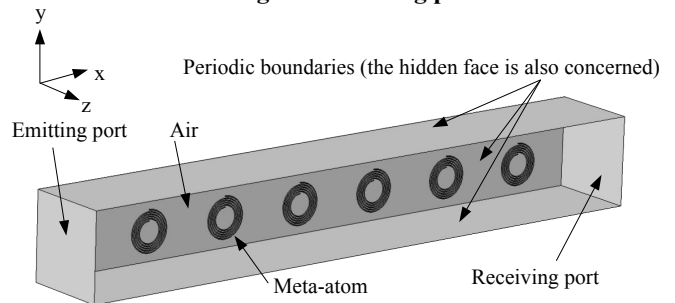


FIG. 3. Configurations for the two kinds of simulation. The first kind is a free space study of a single inclusion surrounded by a Perfectly Matched Layer. We extract the far-field scattered by the inclusion to perform a multipole expansion. The second kind is a study of a whole lattice of meta-atoms using emitting and receiving ports. Fresnel coefficients can be extracted and yield effective values of permittivity and permeability via Clausius-Mossotti formula.

The effective local field may not correspond to Lorentz field, which is assumed to use this formula.

Finally, the chirality of the meta-atom may affect the validity of the constitutive relation given in equation 6. We will discuss that point in the next sections of this paper.

A major benefit of our methodology lies in the fact that only one simulation is required even if we want to study several lattice parameters. Indeed, we only have to modify the volume V of the unit cell in equation 9 to obtain the effective parameters. On the contrary, the Nicolson-Ross method needs a simulation for every lattice parameter. For example, we performed a parametric study on the lattice parameter: 11 different parameters have been tested with both methodologies. The simulation of the first kind required for our multipole expansion was 240 times faster than the parametric study for the Nicolson-Ross method.

However, this model and the Nicolson-Ross method

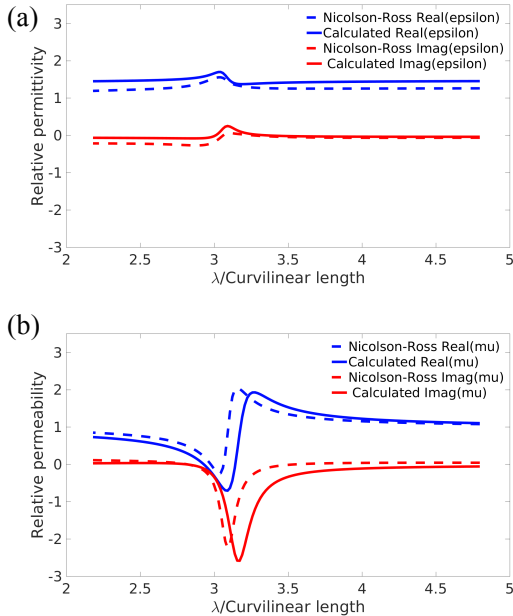


FIG. 4. Comparison of the effective permittivity (a) and permeability (b) obtained with the Nicolson Ross method (dashed curves) and the parameters computed with our methodology (solid curves). The lattice parameter used is 28mm. The global behavior is the same and the calculation seems predictive.

have an important limitation that may partially explain the gap observed between the two approaches: in both methods, we don't take chirality into account. Another drawback of Nicolson-Ross methodology is its inherent mono-incidence and mono-reflection hypothesis. Our method does not suffer from this inconvenience since it relies on the fields radiated in every direction. Moreover, we verify that the dipolar behavior of the inclusion is valid which is consistent with a homogeneity hypothesis of the material. These limitations had no substantial impact on the previous example because the response of the meta-atom to the chosen incoming wave is correctly oriented, as explained in the first section. However, if we want to describe the metamaterial composed of this meta-atom, we have to consider every possible incoming plane-wave. With a different plane wave, our methodology shows limitations.

To illustrate this point, we realized a simulation with an incoming plane wave in which the electric and magnetic fields are oriented along respectively x and y-axis. Currents created along the curved wire generate a magnetic response in the z-direction. Yet, this direction is perpendicular to the background magnetic field. Because of this, the wave propagation in the metamaterial is being disturbed and the classical Nicolson-Ross method and our methodology do not

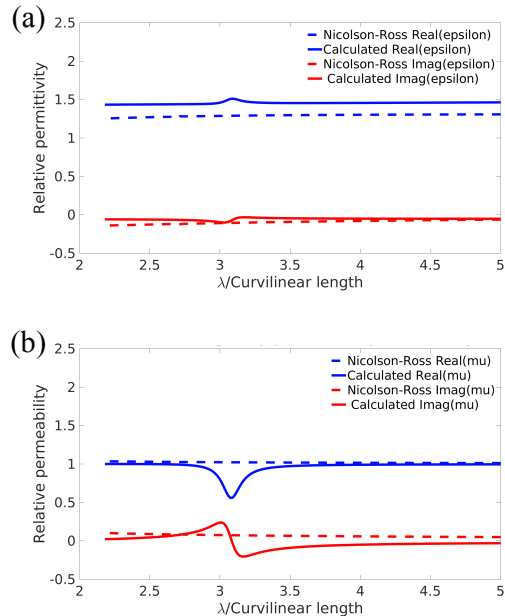


FIG. 5. Comparison of the effective permittivity (a) and permeability (b) obtained with the Nicolson-Ross method (dashed curves) and the parameters computed with our methodology (solid curves) for an excitation wave traveling along the z-direction. The lattice parameter used is 28mm. The global behavior is not well predicted by our methodology because the background magnetic field and the magnetic response of the meta-atoms are not oriented in the same direction. The Nicolson-Ross method does also not give a good response since it does not take the chirality into account.

give similar results, as shown in fig.5. We have to find a more general approach that would give meaningful homogenized parameters for any possible meta-atom, taking into account a more general constitutive relation than the one given in equation 6.

V. EXTENSION TO BI-ANISOTROPIC PARAMETERS EXTRACTION

The assumption we made about the constitutive equation 6 was not correct in the case of an inclusion with strong bi-anisotropic effects. A more general equation given in [35] that can properly describe the physics at stake is the general bi-anisotropic material relation :

$$\begin{pmatrix} \mathbf{D} \\ \mathbf{B} \end{pmatrix} = \begin{pmatrix} \bar{\bar{\epsilon}} & \bar{\bar{a}} \\ \bar{\bar{b}} & \bar{\bar{\mu}} \end{pmatrix} \begin{pmatrix} \mathbf{E} \\ \mathbf{H} \end{pmatrix} \quad (10)$$

With this material relation, 36 different parameters of a 6-by-6 matrix have to be determined for a proper description of the media. We first define the equation describing the polarizability of an atom in this configura-

tion. As the constitutive equation is bi-anisotropic, the polarizability equation takes a similar form.

$$\begin{pmatrix} \mathbf{p} \\ \mathbf{m} \end{pmatrix} = \begin{pmatrix} \bar{\alpha}_e & \bar{\alpha}_{em} \\ \bar{\alpha}_{me} & \bar{\alpha}_m \end{pmatrix} \begin{pmatrix} \mathbf{E}_{\text{loc}} \\ \mathbf{B}_{\text{loc}} \end{pmatrix} \quad (11)$$

The vector on the left-hand side is a 6-by-1 vector composed of the coefficients of the electric and magnetic dipoles. \mathbf{E}_{loc} and \mathbf{B}_{loc} correspond respectively to the local electric and magnetic field applied to the meta-atom. The first objective consists in finding the 36 different coefficients of the polarizability tensor which describe the response of the atom to external fields. With a single simulation of a background plane wave, we cannot determine these coefficients. We have to enlighten the meta-atom in several different ways to obtain enough information about its scattering properties. With six different excitation plane wave configurations we can build from equation 11 a new matrix equation:

$$\bar{\mathbf{R}} = \begin{pmatrix} \bar{\alpha}_e & \bar{\alpha}_{em} \\ \bar{\alpha}_{me} & \bar{\alpha}_m \end{pmatrix} \bar{\mathbf{S}} \quad (12)$$

with

$$\bar{\mathbf{R}} = \begin{pmatrix} p_x^1 & p_x^2 & p_x^3 & p_x^4 & p_x^5 & p_x^6 \\ p_y^1 & p_y^2 & p_y^3 & p_y^4 & p_y^5 & p_y^6 \\ p_z^1 & p_z^2 & p_z^3 & p_z^4 & p_z^5 & p_z^6 \\ m_x^1 & m_x^2 & m_x^3 & m_x^4 & m_x^5 & m_x^6 \\ m_y^1 & m_y^2 & m_y^3 & m_y^4 & m_y^5 & m_y^6 \\ m_z^1 & m_z^2 & m_z^3 & m_z^4 & m_z^5 & m_z^6 \end{pmatrix} \quad (13)$$

$$\bar{\mathbf{S}} = \begin{pmatrix} E_x^1 & E_x^2 & E_x^3 & E_x^4 & E_x^5 & E_x^6 \\ E_y^1 & E_y^2 & E_y^3 & E_y^4 & E_y^5 & E_y^6 \\ E_z^1 & E_z^2 & E_z^3 & E_z^4 & E_z^5 & E_z^6 \\ B_x^1 & B_x^2 & B_x^3 & B_x^4 & B_x^5 & B_x^6 \\ B_y^1 & B_y^2 & B_y^3 & B_y^4 & B_y^5 & B_y^6 \\ B_z^1 & B_z^2 & B_z^3 & B_z^4 & B_z^5 & B_z^6 \end{pmatrix}$$

S- and R-matrix are defined by the concatenation of the vectors of the 6 different simulations. R is the reaction matrix defined for i=1 to 3 by $R_{ij} = p_j^i$ and for i=4 to 6 by $R_{ij} = m_j^i$, noting p_j^i and m_j^i the j^{th} electric and magnetic dipole coefficients of the i^{th} simulation. S is the source matrix defined for i=1 to 3 by $R_{ij} = E_j^i$ and for i=4 to 6 by $R_{ij} = B_j^i$, noting E_j^i and B_j^i the j^{th} electric and magnetic local field component of the i^{th} simulation.

As we study single meta-atoms in free space, the local fields required in equation 11 are equal to the background fields we define for the simulation. Moreover, every plane wave of the set we use has to be linearly independent of the five others so that the S-matrix is invertible. As we only use linearly polarized waves in the (x, y, z) coordinate system, this matrix can be simplified:

$$\bar{\mathbf{S}} = \frac{E_b}{c} \begin{pmatrix} c & c & 0 & 0 & 0 & 0 \\ 0 & 0 & c & c & 0 & 0 \\ 0 & 0 & 0 & 0 & c & c \\ 0 & 0 & 1 & 0 & 1 & 0 \\ 1 & 0 & 0 & 0 & 0 & -1 \\ 0 & -1 & 0 & -1 & 0 & 0 \end{pmatrix} \quad (14)$$

E_b is the amplitude of the background electric field of the wave and c is the free-space speed of light. We verify numerically that this S-matrix is invertible: with these 6 excitation conditions, we have enough information to determine every unknown material parameter. The R-matrix is obtained by extraction of the dipole moments for each of the 6 different simulations, using the methodology described by inversion of equation 3. Thanks to equation 12, a simple inversion of the S-matrix gives the polarizability tensor of the meta-atom. Since we have access to the bi-anisotropic polarizability of our particle, we have now to link it to the macroscopic material properties of a whole lattice described by the constitutive equation 10.

First, we have to write equation 12 to link the electric and magnetic dipole responses to the actual background field in the general case. Indeed, if we consider a whole lattice of the meta-atom, the background fields won't be equal to the local fields as for the single meta-atom. We want to create an analog of the Clausius-Mossotti relation for bi-anisotropic materials, so we consider that the local electric field is the field inside a charged Lorentz sphere:

$$\mathbf{E}_{\text{loc}} = \mathbf{E}_b + \frac{\mathbf{P}}{3\epsilon_0} \quad (15)$$

with \mathbf{P} the electric polarization of the medium. In ref.[34], an analog for the magnetic field is given :

$$\mathbf{B}_{\text{loc}} = \mathbf{B}_b - \frac{2\mu_0\mathbf{M}}{3} \quad (16)$$

Electric and magnetic polarization can be linked to electric and magnetic dipole moments and the volume V of a unit cell containing the meta-atom :

$$\mathbf{P} = \frac{\mathbf{p}}{V} \quad (17)$$

$$\mathbf{M} = \frac{\mathbf{m}}{V}$$

The local fields can be replaced in equation 11 using equations 15 and 16:

$$\begin{pmatrix} \mathbf{p} \\ \mathbf{m} \end{pmatrix} = \begin{pmatrix} \bar{\alpha}_e & \bar{\alpha}_{em} \\ \bar{\alpha}_{me} & \bar{\alpha}_m \end{pmatrix} \begin{pmatrix} \mathbf{E}_b + \frac{\mathbf{p}}{3V\epsilon_0} \\ \mathbf{B}_b - \frac{2\mu_0\mathbf{m}}{3V} \end{pmatrix} \quad (18)$$

After a few manipulations of equation 18, we obtain an equation giving the electric and magnetic dipoles as a function of the background fields:

$$\begin{pmatrix} \mathbf{p} \\ \mathbf{m} \end{pmatrix} = \left[\bar{I}_6 - \begin{pmatrix} \bar{\alpha}_e & \bar{\alpha}_{em} \\ \bar{\alpha}_{me} & \bar{\alpha}_m \end{pmatrix} \begin{pmatrix} \frac{1}{3V\epsilon_0}\bar{I}_3 & 0 \\ 0 & -\frac{2\mu_0}{3V}\bar{I}_3 \end{pmatrix} \right]^{-1} \begin{pmatrix} \bar{\alpha}_e & \bar{\alpha}_{em} \\ \bar{\alpha}_{me} & \bar{\alpha}_m \end{pmatrix} \begin{pmatrix} \mathbf{E}_b \\ \mathbf{B}_b \end{pmatrix} \quad (19)$$

In this matrix equation, we give the link between the dipoles and the background fields: the local fields are similar to the Lorentz fields inside a charged sphere. We obtain a relation between the macroscopic background field and the microscopic dipole moments of the meta-atoms. To manipulate easily this equation later in this paper, we introduce a modified polarisability tensor:

$$\begin{pmatrix} \mathbf{p} \\ \mathbf{m} \end{pmatrix} = \begin{pmatrix} \bar{\alpha}'_e & \bar{\alpha}'_{em} \\ \bar{\alpha}'_{me} & \bar{\alpha}'_m \end{pmatrix} \begin{pmatrix} \mathbf{E}_b \\ \mathbf{B}_b \end{pmatrix} \quad (20)$$

The coefficients of this new polarizability tensor can be obtained by identification with equation 19. It is straightforward to prove that as volume V of the unit cell increases, the polarizability tensor defined in 20 converges to the classical polarizability tensor.

$$\begin{pmatrix} \bar{\alpha}'_e & \bar{\alpha}'_{em} \\ \bar{\alpha}'_{me} & \bar{\alpha}'_m \end{pmatrix} \xrightarrow{V \rightarrow +\infty} \begin{pmatrix} \bar{\alpha}_e & \bar{\alpha}_{em} \\ \bar{\alpha}_{me} & \bar{\alpha}_m \end{pmatrix} \quad (21)$$

$$\frac{1}{V} \begin{pmatrix} \mathbf{p} \\ \mathbf{m} \end{pmatrix} = \begin{pmatrix} \epsilon_0 \left(\bar{\chi}_e - \bar{\chi}_{em} \left(\bar{I}_3 + \bar{\chi}_m \right)^{-1} \bar{\chi}_{me} \right) & \frac{\epsilon_0}{\mu_0} \bar{\chi}_{em} \left(\bar{I}_3 + \bar{\chi}_m \right)^{-1} \\ \bar{\chi}_{me} - \bar{\chi}_m \left(\bar{I}_3 + \bar{\chi}_m \right)^{-1} \bar{\chi}_{me} & \frac{\bar{\chi}_m}{\mu_0} \left(\bar{I}_3 + \bar{\chi}_m \right)^{-1} \end{pmatrix} \begin{pmatrix} \mathbf{E}_b \\ \mathbf{B}_b \end{pmatrix} \quad (26)$$

Equations 19 and 26 both link the microscopic dipole response of a meta-atom with the external background field. We perform a block-by-block identification to obtain the susceptibility tensors. After a few calculations, it is possible to express each block of susceptibility as a function of the modified polarizability blocks defined in 20:

Equation 21 expresses the fact that if the meta-atom density is very low in the metamaterial, the effect of the neighbors becomes insignificant. Background fields and local fields applied to the meta-atom are approximately equal in that case. The next step consists in finding a similar equation, linking dipoles and background fields, involving macroscopic parameters instead of the microscopic polarizability. We now consider that the global response of the bi-anisotropic material is described by susceptibility tensors:

$$\begin{aligned} \mathbf{P} &= \epsilon_0 \bar{\chi}_e \mathbf{E}_b + \epsilon_0 \bar{\chi}_{em} \mathbf{H}_b \\ \mathbf{M} &= \bar{\chi}_m \mathbf{H}_b + \bar{\chi}_{me} \mathbf{E}_b \end{aligned} \quad (22)$$

These formulae express susceptibility tensors as functions of the background global fields. We now have to replace \mathbf{H}_b with \mathbf{B}_b to perform an identification using formula 19. We easily obtain the link between these two fields considering the constitutive equation 10:

$$\mathbf{B}_b = \bar{b} \mathbf{E}_b + \bar{\mu} \mathbf{H}_b \quad (23)$$

this can be rewritten:

$$\mathbf{B}_b = \mu_0 \bar{\chi}_{me} \mathbf{E}_b + \mu_0 \left(\bar{I}_3 + \bar{\chi}_m \right) \mathbf{H}_b \quad (24)$$

We then write \mathbf{H}_b as a function of \mathbf{B}_b and \mathbf{E}_b :

$$\mathbf{H}_b = \frac{1}{\mu_0} \left(\bar{I}_3 + \bar{\chi}_m \right)^{-1} \left(\mathbf{B}_b - \mu_0 \bar{\chi}_{me} \mathbf{E}_b \right) \quad (25)$$

We replace \mathbf{H}_b with expression 25 in equation 22, and write the equation system as a matrix equation:

$$\text{Block 22 : } \bar{\chi}_m = \left(\bar{I}_3 - \frac{\mu_0}{V} \bar{\alpha}'_m \right)^{-1} \frac{\mu_0}{V} \bar{\alpha}'_m$$

$$\text{Block 12 : } \bar{\chi}_{em} = \frac{\mu_0}{\epsilon_0 V} \bar{\alpha}'_{em} \left(\bar{I}_3 + \bar{\chi}_m \right)$$

$$\text{Block 21 : } \bar{\chi}_{me} = \left[\bar{I}_3 - \bar{\chi}_m \left(\bar{I}_3 + \bar{\chi}_m \right)^{-1} \right]^{-1} \frac{\bar{\alpha}'_{me}}{V}$$

$$\text{Block 11 : } \bar{\chi}_e = \frac{\bar{\alpha}'_e}{V \epsilon_0} + \bar{\chi}_{em} \left(\bar{I}_3 + \bar{\chi}_m \right)^{-1} \bar{\chi}_{me} \quad (27)$$

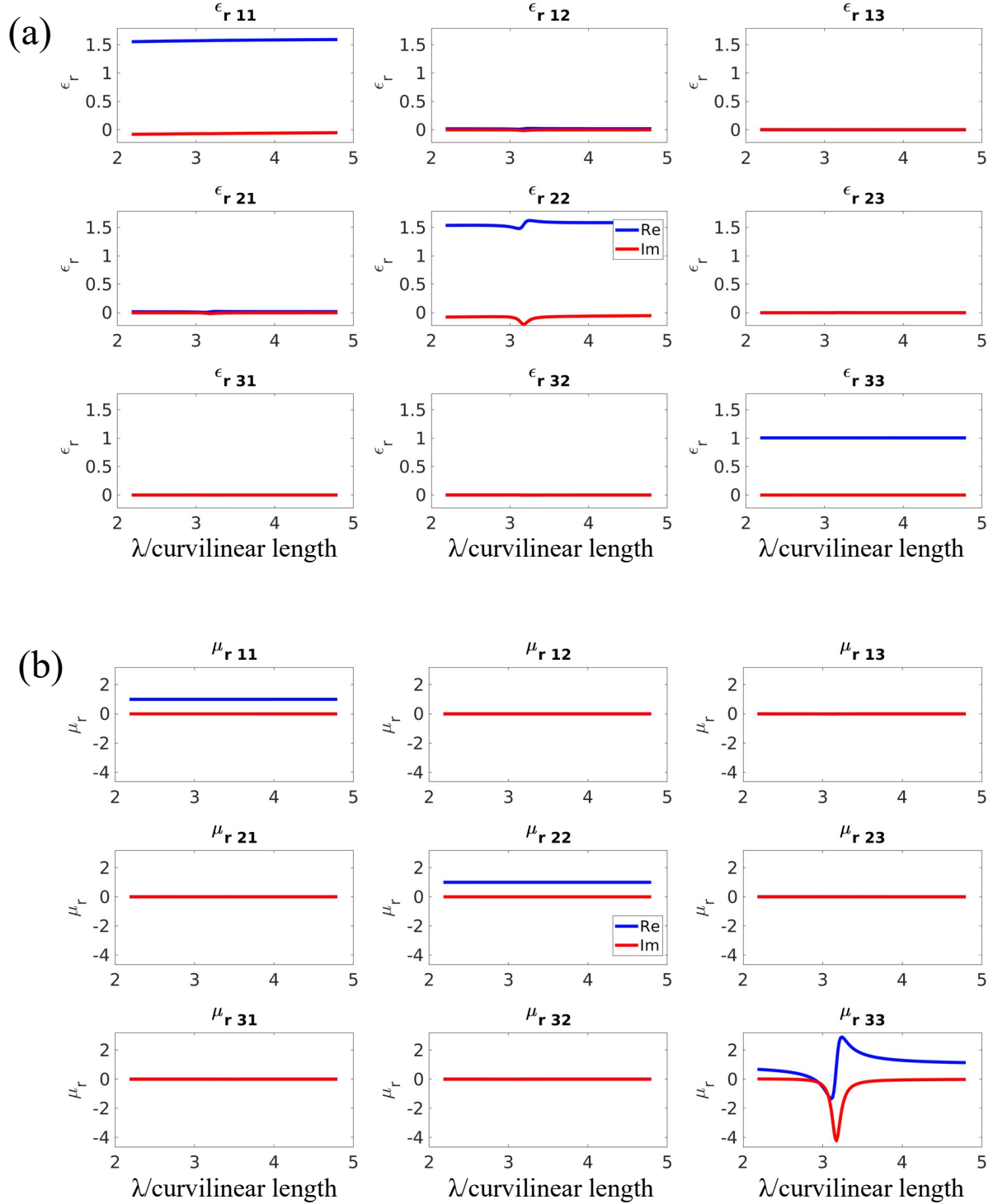


FIG. 6. Relative permittivity (a) and permeability tensors (b) for the spiral. As predicted in [27], components 13, 23, 31 and 32 are close to zero in both matrices. Permittivity takes values above unity in the x- and y- directions and unity in the z-direction. Permeability is almost equal to the 3-by-3 identity-matrix except for its 33-component: a Lorentz resonance appears. This metamaterial can behave as an MNZ material near its first frequency of resonance. We use the same horizontal and vertical ranges for every panel to facilitate the comparison between the different matrix components.

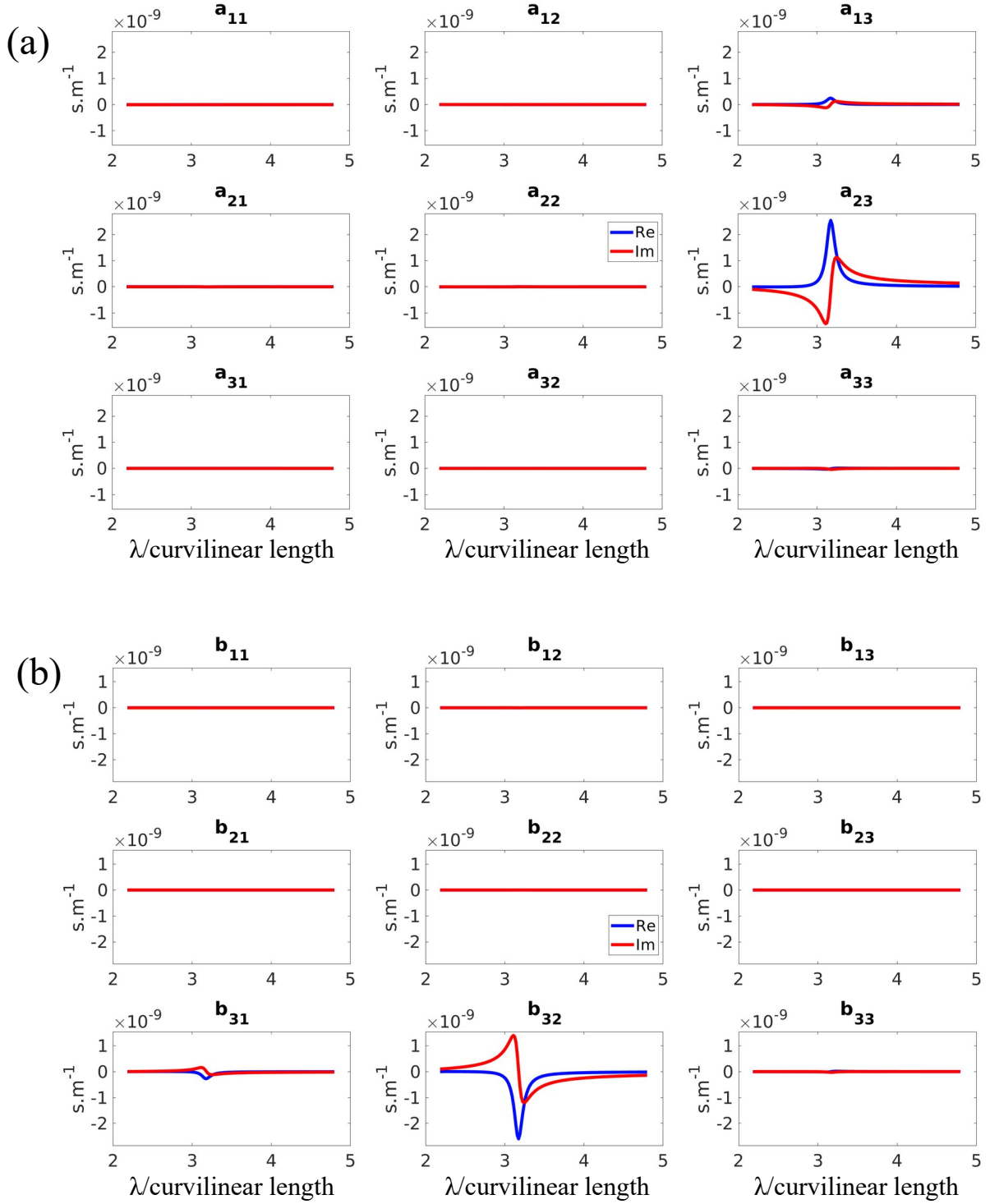


FIG. 7. a-tensor (a) and b-tensor (b) parameters for the spiral. Reference [27] predicted that these parameters are equal to zero except for components 13 and 23 of the a-tensor and components 31 and 32 for the b-tensor. Moreover, the Onsager-Casimir relations are respected as we verify the relations : $a_{13} = -b_{31}$ and $a_{23} = -b_{32}$. We verify reciprocity for this metamaterial. We use the same horizontal and vertical ranges for every panel to facilitate the comparison between the different matrix components.

The first block to calculate is block 22, to obtain the $\bar{\bar{\chi}}_m$ susceptibility that is required for the calculation of the other blocks. We then compute block 12 and 21 to obtain $\bar{\bar{\chi}}_{em}$ and $\bar{\bar{\chi}}_{me}$. Finally, block 11 can be calculated. The last step consists in the calculation of the permittivity, permeability and chirality tensors using the relations given in equation 28:

$$\begin{aligned}\bar{\bar{\epsilon}} &= \epsilon_0 \left(\bar{\bar{I}}_3 + \bar{\bar{\chi}}_e \right) \\ \bar{\bar{\mu}} &= \mu_0 \left(\bar{\bar{I}}_3 + \bar{\bar{\chi}}_m \right) \\ \bar{\bar{a}} &= \epsilon_0 \bar{\bar{\chi}}_{em} \\ \bar{\bar{b}} &= \mu_0 \bar{\bar{\chi}}_{me}\end{aligned}\quad (28)$$

In this section, we found an analog to the Clausius-Mossotti relation that is valid for every bi-anisotropic material as long as it satisfies the constitutive relation 10. Using this relation we can perform a parameter calculation of a full bi-anisotropic metamaterial the same way we performed it for regular magneto-dielectric. The simulation of a single meta-atom in free space under different enlightenment conditions gives enough information to characterize the macroscopic behavior of a whole lattice.

VI. VALIDATION OF THE BI-ANISOTROPIC EXTRACTION

We study the meta-atom presented in section 4 to realize the full bi-anisotropic parameters calculation. We use the configuration of fig.3 for the full-wave simulation, where the meta-atom is surrounded by a Perfectly Matched Layer playing the role of infinite free-space.

Assuming a lattice parameter of 2.8cm, this methodology leads to a tensor description of the metamaterial over a whole frequency range. This study is made around the first frequency of resonance of the structure, for 151 different frequencies. We give in fig.6 the results for the relative permittivity and permeability and in fig.7 those for the a- and b-parameters. Fig.6 shows a strong magnetic behavior along the z-direction. Indeed, the real part of the permeability gets negative values at the resonance. It allows us to imagine a Mu-Near-Zero (MNZ) behavior for this metamaterial for a frequency range close to the frequency of resonance. The mathematical study published by Isik and Esselle [27] describes the bi-anisotropic behavior of monofilar, bifilar, trifilar and quadrifilar spiral metamaterial. We study here a monofilar spiral and our

bi-anisotropic response fits perfectly with what was expected. According to this paper, the material property-tensor for a monofilar spiral takes the form given in equation 29:

$$\begin{pmatrix} \bar{\bar{\epsilon}} & \bar{\bar{a}} \\ \bar{\bar{b}} & \bar{\bar{\mu}} \end{pmatrix} = \begin{pmatrix} \epsilon_0 \epsilon_{r11} & \epsilon_0 \epsilon_{r12} & 0 & 0 & 0 & a_{13} \\ \epsilon_0 \epsilon_{r21} & \epsilon_0 \epsilon_{r22} & 0 & 0 & 0 & a_{23} \\ 0 & 0 & \epsilon_0 \epsilon_{r33} & 0 & 0 & 0 \\ 0 & 0 & 0 & \mu_0 \mu_{r11} & \mu_0 \mu_{r12} & 0 \\ 0 & 0 & 0 & \mu_0 \mu_{r21} & \mu_0 \mu_{r22} & 0 \\ b_{31} & b_{31} & 0 & 0 & 0 & \mu_0 \mu_{r33} \end{pmatrix}\quad (29)$$

Our results fully agree with this 6-by-6 property tensor and the predictions made in [27]. Moreover, these results are also coherent with the Onsager-Casimir principle [36] [37] [38] that predicts a relation between the a- and b-tensors:

$$\bar{\bar{a}} = -\bar{\bar{b}}^T \quad (30)$$

We observe on fig7 that $a_{13} = -b_{31}$ and $a_{23} = -b_{32}$ over the whole frequency range, whereas all the other components are negligible compared to these four ones. The compatibility of our results with the computations made in [27] and with the Onsager-Casimir reciprocal principle constitutes a validation of our method.

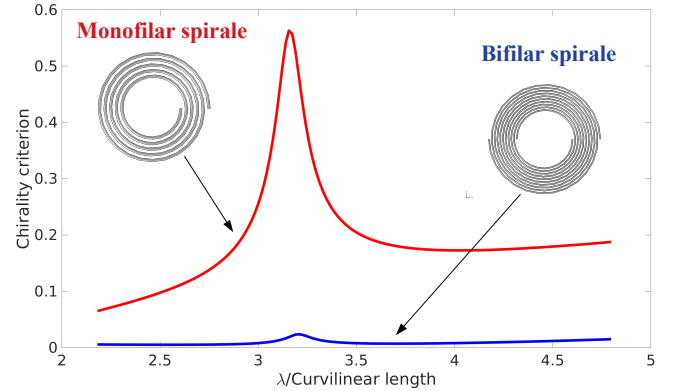


FIG. 8. Chirality criterion for the monofilar and bifilar spirals. We see that at the frequency of resonance the chirality criterion is very high for the monofilar spiral. Chirality represents up to 55% of the meta-atom response. The criterion remains very low for the bifilar spiral and does not exceed 3%.

Creating a validation tool for the properties of metamaterials is one of the main objectives of this bi-anisotropic study. Properties required for specific applications such as the super-lens or invisibility cloaks need to be validated via a strong approach: we cannot settle for an approach where chirality is assimilated to permeability or permittivity. We build a criterion to measure the chirality strength of the metamaterial. The effects of the spatial dispersion are encoded in this far-field response. We suggest the criterion provided in equation 31. This criterion measures the strength of the chiral

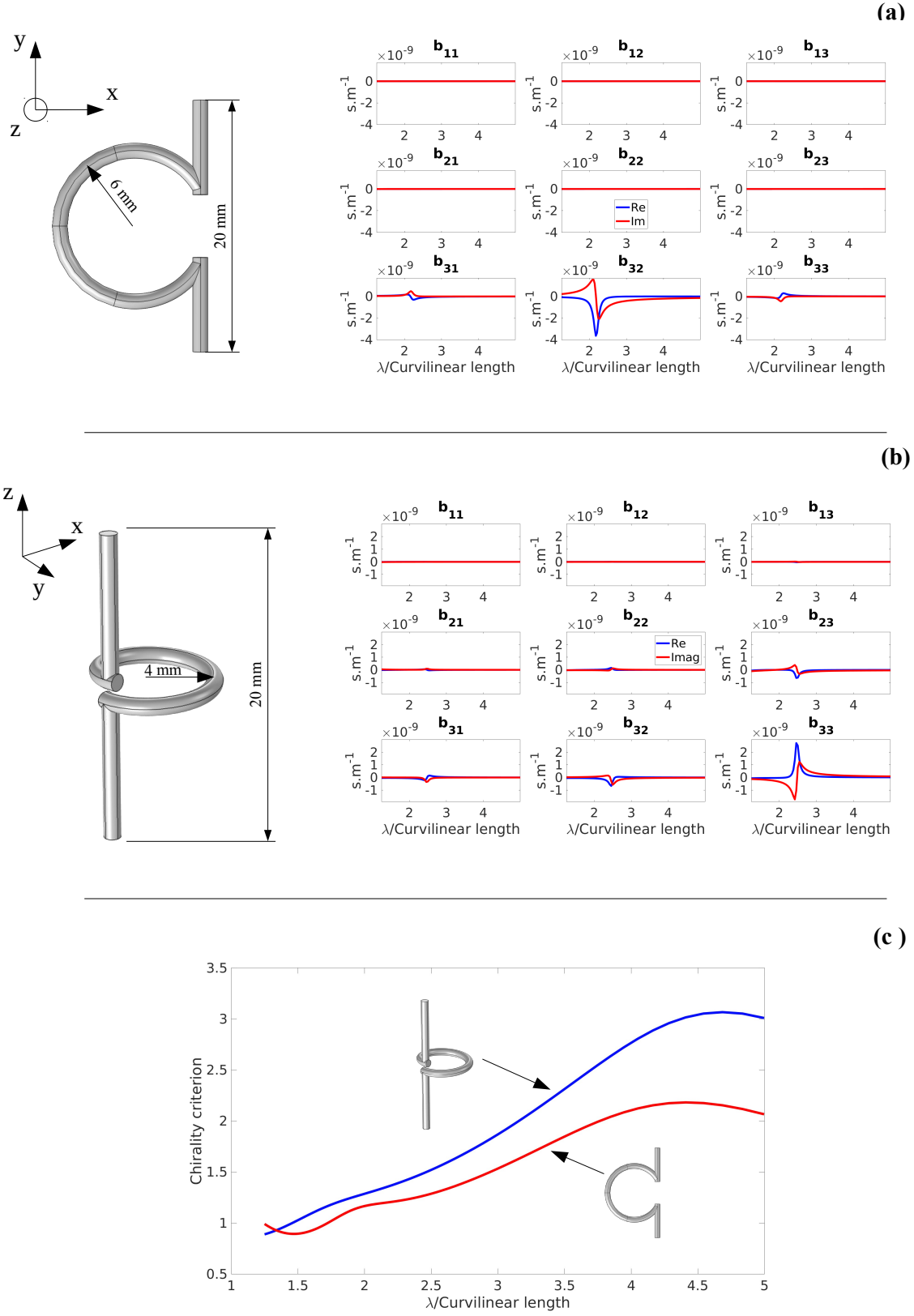


FIG. 9. Geometry and b -matrix for an Omega-particle (a) and a twisted Omega-particle (b). We also give the chirality criterion (c), which is high (superior to 1) for both particles. As we can see, the preponderant coefficient depends on the geometry of the particle. For the Omega-particle, an electric excitation along the y -axis is responsible for an important magnetic response along z -axis. For the twisted Omega-particle, an electric excitation along the z -axis is responsible for an important magnetic response also along z -axis.

response compared to the regular magneto-dielectric response of the meta-atom.

$$C = \frac{1}{2} \left(\frac{1}{Z_0} \frac{\|\bar{\chi}_{em}\|}{\|\bar{\chi}_e\|} + Z_0 \frac{\|\bar{\chi}_{me}\|}{\|\bar{\chi}_m\|} \right) \quad (31)$$

The first term of the sum compares the weight of the chiral electric response to the regular dielectric response of the metamaterial, whereas the second term compares the chiral magnetic response to the regular magnetic response. We define the criterion as the arithmetic mean of these two terms. The norm used for the susceptibility tensors is the Frobenius norm for matrix, given in equation 32:

$$\|A\| = \sqrt{\text{trace}(A^*A)} \quad (32)$$

where A^* is the conjugate of the transpose matrix.

In reference [39], authors define a local chirality criterion taking into account the local spatial dispersion in optical metamaterials. On the contrary, our approach leads to an effective chirality criterion taking into account every possible direction of incidence. The computation of this criterion has been realized for the monofilar spiral and also for a bifilar spiral. We can observe in fig.8 that the criterion is very high for the monofilar, whereas it is very close to zero for the bifilar, as predicted by Isik and Esselle in [27]. We can conclude that the bifilar spiral may be a good candidate for the design of an MNZ metamaterial whereas it is risky to use the monofilar spiral because of non-negligible chiral effects. In the realization of an electromagnetic device such as the super-lens or an invisibility cloak, it is important to know the whole permittivity and permeability tensors of the metamaterial. Our approach gives both permittivity and permeability tensors and also give a criterion that quantifies the chirality of the meta-atom: every required piece of information is available.

This criterion can also be applied to state-of-the-art chiral particles. The most common particles exhibiting a high chirality are certainly the omega-particle and the twisted omega-particle [40] [41]. We performed the whole methodology for these two meta-atoms: geometry, a-tensors and chirality criterion for both particles are given in figure 9.

We have to pay particular attention to the dipole expansion of such particles: as the omega-particle is not really small compared to the wavelength around the first frequency of resonance, quadrupole moments can impact the accuracy of the dipole model. The relative error of the dipole approximation estimated thanks to the evaluation index defined in equation 4 gives a maximum 10% error near the frequency of resonance for both

particles. We have to keep in mind that quadrupole and higher-order moments may partially invalidate the hypothesis made to develop our methodology.

As we can see, the b_{32} coefficient for the omega-particle is preponderant, showing the link between the electric excitation along the y-axis and the magnetic response along the z-axis. On the contrary, the b_{33} coefficient is preponderant for the twisted omega-particle, showing the link between the electric excitation along the y-axis and the magnetic response along the y-axis. These results are in good agreement with the literature [35].

VII. CONCLUSION

Summary of the methodology

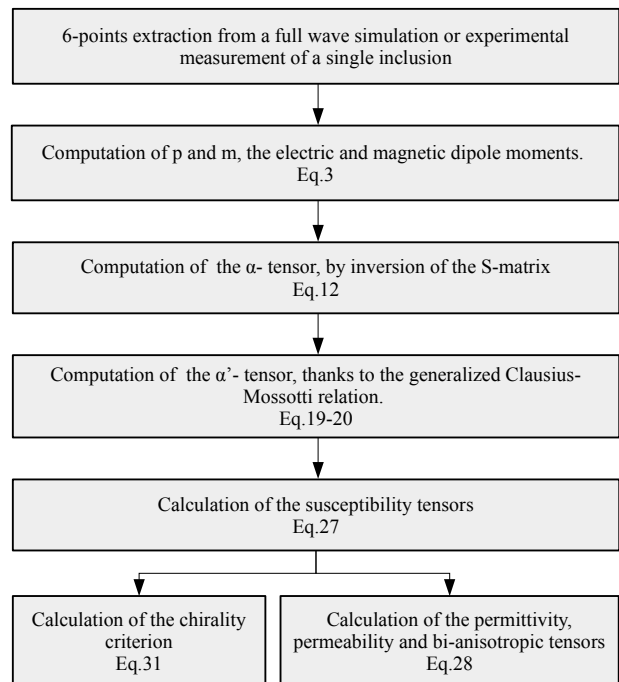


FIG. 10. Description of the bi-anisotropic homogenization methodology based on a Clausius-Mossotti generalization.

We demonstrate in this article that a few free-space simulations of a single meta-atom can give an important amount of information about an array of this inclusion. Thanks to the 6-points extraction, it is possible to calculate the electric and magnetic dipoles the particle exhibits. By then performing simulations with different polarizations and incidence angles, we compute the 36 components of the bi-anisotropic polarizability tensors. To obtain suitable susceptibility tensors we establish a generalized Clausius-Mossotti relation for bi-anisotropic materials. Finally, we find permittivity and permeability tensors and we define a chirality criterion. The whole

method is summarized in fig.10.

This methodology could also employ experimental measures of the field scattered by a meta-atom. Nothing would change in the computation except that the far-field scattered by the meta-atom would come from the experience instead of a full-wave simulation.

Our approach is very convenient in the study of metamaterial because it gives precise information about its behavior thanks to the study of a single particle in free

space. It is also convenient for the study of miniaturized meta-atoms, for which meshes are sometimes difficult to realize. Computation costs in terms of time and processor capacity are reduced in comparison with the study of a whole lattice. We can study a substantial number of meta-atom designs. It also predicts the behavior of the associated metamaterial and helps us to choose the best designs required for any specific application. Depending on the application, our method can either be useful to prevent chiral effects or to amplify it when designing metamaterials.

-
- [1] J. B. Pendry, *Physical Review Letters* **85**, 3966 (2000).
- [2] J. B. Pendry, D. Schurig, and D. R. Smith, *Science* **312**, 1780 (2006).
- [3] U. Leonhardt and T. G. Philbin, *New Journal of Physics* **8**, 247 (2006).
- [4] W. Cai, U. K. Chettiar, A. V. Kildishev, and V. M. Shalaev, *Nature Photonics* **1**, 224 (2007).
- [5] S. Hrabar, I. Krois, and A. Kiricenko, *Metamaterials-2009 Congress in London*, **4**, 89 (2010).
- [6] A. M. Nicolson and G. F. Ross, *IEEE Transactions on Instrumentation and Measurement* **19**, 377 (1970).
- [7] O. Luukkonen, S. I. Maslovski, and S. A. Tretyakov, *IEEE Antennas and Wireless Propagation Letters* **10**, 1295 (2011).
- [8] A. L. d. Paula, M. C. Rezende, and J. J. Barroso, in *2011 SBMO/IEEE MTT-S International Microwave and Optoelectronics Conference (IMOC 2011)* (2011) pp. 488–492.
- [9] D. R. Smith, D. C. Vier, T. Koschny, and C. M. Soukoulis, *Physical Review E* **71** (2005), 10.1103/PhysRevE.71.036617.
- [10] E. J. Rothwell, J. L. Frasc, S. M. Ellison, P. Chahal, and R. O. Ouedraogo, *Progress In Electromagnetics Research* **157**, 31 (2016), publisher: Electromagnetics Academy.
- [11] D. R. Smith and J. B. Pendry, *JOSA B* **23**, 391 (2006).
- [12] J.-M. Lerat, N. Malléjac, and O. Acher, *Journal of Applied Physics* **100**, 084908 (2006).
- [13] C. R. Simovski, *Journal of Optics* **13**, 013001 (2011).
- [14] A. Alù, *Physical Review B* **83** (2011), 10.1103/PhysRevB.83.081102.
- [15] T. G. Mackay and A. Lakhtakia, *SPIE Reviews* **1**, 018003 (2010).
- [16] S. Zhang, Y.-S. Park, J. Li, X. Lu, W. Zhang, and X. Zhang, *Physical Review Letters* **102**, 023901 (2009).
- [17] M. C. K. Wiltshire, J. B. Pendry, and J. V. Hajnal, *Journal of Physics: Condensed Matter* **21**, 292201 (2009).
- [18] T. G. Mackay, A. Lakhtakia, and W. S. Weighofer, *Physical Review E* **62**, 6052 (2000).
- [19] O. Ouchetto, C. Qiu, S. Zouhdi, L. Li, and A. Razek, *IEEE Transactions on Microwave Theory and Techniques* **54**, 3893 (2006).
- [20] D. Cohen and R. Shavit, *IEEE Transactions on Antennas and Propagation* **63**, 2071 (2015).
- [21] A. Ciattoni and C. Rizza, *Physical Review B* **91** (2015), 10.1103/PhysRevB.91.184207.
- [22] S. Mühlig, C. Menzel, C. Rockstuhl, and F. Lederer, *Metamaterials Metamaterials Congress - 2010*, **5**, 64 (2011).
- [23] Y. Zeng, C. Dineen, and J. V. Moloney, *Physical Review B* **81**, 075116 (2010).
- [24] D. J. Cho, F. Wang, X. Zhang, and Y. R. Shen, *Physical Review B* **78**, 121101 (2008).
- [25] A. Alù, *Physical Review B* **84** (2011), 10.1103/PhysRevB.84.075153.
- [26] G. Klotz, N. Mallejac, and S. Enoch, *ICEAA 2019* (2019).
- [27] O. Isik and K. P. Esselle, *Metamaterials* **3**, 33 (2009).
- [28] J. D. Jackson, (1962).
- [29] F. Bilotti, A. Toscano, and L. Vegni, *IEEE Transactions on Antennas and Propagation* **55**, 2258 (2007).
- [30] D. Zarifi, M. Soleimani, V. Nayyeri, and J. Rashed-Mohassel, *IEEE Transactions on Antennas and Propagation* **60**, 5768 (2012).
- [31] J. Krupka, W. Strupinski, and N. Kwietniewski, *Journal of Nanoscience and Nanotechnology* **11**, 3358 (2011).
- [32] F. Bilotti, A. Toscano, L. Vegni, K. Aydin, K. B. Alici, and E. Ozbay, *IEEE Transactions on Microwave Theory and Techniques* **55**, 2865 (2007).
- [33] C. R. Simovski and S. A. Tretyakov, *Physical Review B* **75**, 195111 (2007).
- [34] A. Niranjana and B. K. Padhi, *Physics Education* **30**, 7 (2014).
- [35] A. Serdyukov, I. Semchenko, S. Tretyakov, and A. Sihvola, (2001).
- [36] L. Onsager, *Physical Review* **37**, 405 (1931).
- [37] G. T. Rado, *Physical Review B* **8**, 5239 (1973).
- [38] S. Tretyakov, A. Sihvola, and B. Janczewicz, *Journal of Electromagnetic Waves and Applications* **16**, 573 (2002).
- [39] Y. Tang and A. E. Cohen, *Physical Review Letters* **104**, 163901 (2010), publisher: American Physical Society.
- [40] C. Caloz and A. Sihvola, arXiv:1903.09087 [physics] (2019), arXiv: 1903.09087.
- [41] I. Fernandez-Corbaton, M. Fruhnert, and C. Rockstuhl, *Physical Review X* **6**, 031013 (2016).